Brief communication

Cell Chemical Biology

N-acetyl-L-cysteine averts ferroptosis by fostering glutathione peroxidase 4

Graphical abstract

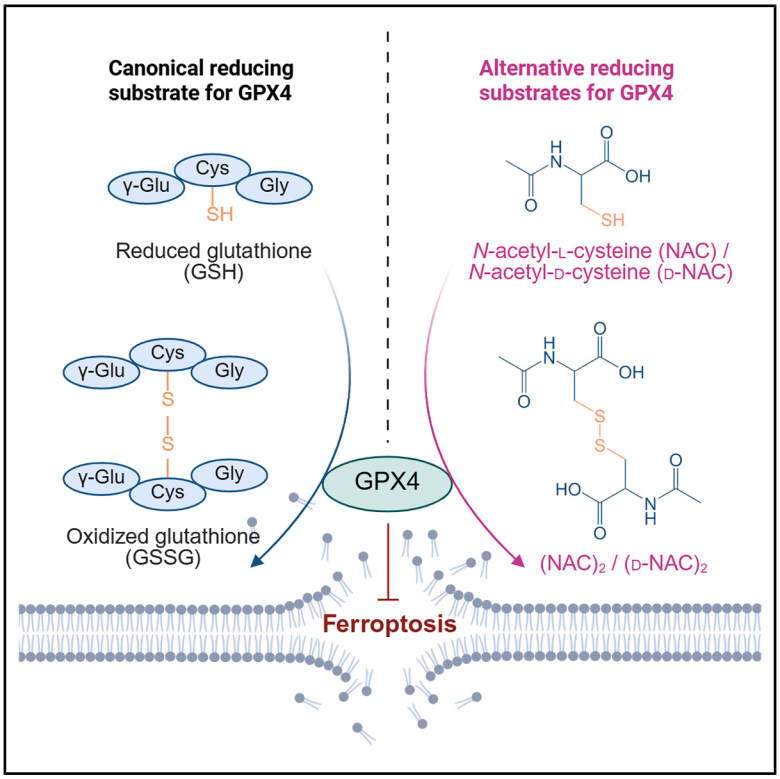

Highlights

- NAC and D-NAC inhibit ferroptosis independently of cellular GSH
- The presence of GPX4 is a prerequisite for NAC and D-NAC to inhibit ferroptosis
- NAC and its enantiomer D-NAC are direct reducing substrates of GPX4
- GPX4 exploits diverse reducing substrates to reduce lipid hydroperoxides *in vitro*

Authors

Jiashuo Zheng (郑嘉烁), Weijia Zhang (张唯佳), Junya Ito, Bernhard Henkelmann, Chenxi Xu (徐晨曦), Eikan Mishima, Marcus Conrad

Correspondence

marcus.conrad@helmholtz-munich.de

In brief

Zheng and Zhang et al. identify *N*-acetyl-L-cysteine (NAC) and its enantiomer *N*-acetyl-D-cysteine (D-NAC) as direct reducing substrates of glutathione peroxidase 4 (GPX4). They further reveal a broad range of reducing substrates for GPX4 *in vitro*. This study suggests GPX4 may utilize other reducing substrates to counteract ferroptosis upon glutathione deficiency.

Zheng et al., 2025, Cell Chemical Biology *32*, 1–9
May 15, 2025
https://doi.org/10.1016/j.chembiol.2025.04.002

CellPress

Please cite this article in press as: Zheng et al., *N*-acetyl-L-cysteine averts ferroptosis by fostering glutathione peroxidase 4, Cell Chemical Biology (2025), https://doi.org/10.1016/j.chembiol.2025.04.002

Cell Chemical Biology

CellPress
OPEN ACCESS

Brief communication

N-acetyl-L-cysteine averts ferroptosis by fostering glutathione peroxidase 4

Jiashuo Zheng (郑嘉烁),[1,5] Weijia Zhang (张唯佳),[1,5] Junya Ito,[1,2] Bernhard Henkelmann,[1] Chenxi Xu (徐晨曦),[1] Eikan Mishima,[1,3] and Marcus Conrad[1,4,6,*]

[1]Helmholtz Zentrum München, Institute of Metabolism and Cell Death, Molecular Targets and Therapeutics Center, 85764 Neuherberg, Germany
[2]Laboratory of Food Function Analysis, Tohoku University Graduate School of Agricultural Science, Sendai, Miyagi 980-8572, Japan
[3]Division of Nephrology, Rheumatology and Endocrinology, Tohoku University Graduate School of Medicine, Sendai, Miyagi 980-8574, Japan
[4]Translational Redox Biology, Technical University of Munich (TUM), TUM Natural School of Sciences, 85748 Garching, Germany
[5]These authors contributed equally
[6]Lead contact
*Correspondence: marcus.conrad@helmholtz-munich.de
https://doi.org/10.1016/j.chembiol.2025.04.002

SIGNIFICANCE Ferroptosis, a distinct form of cell death, has garnered significant attention as both a potential strategy for eradicating cancer cells and a target for therapeutic inhibition in various diseases. Among the rapidly expanding body of research on ferroptosis, *N*-acetyl-L-cysteine (NAC) is frequently employed as a ferroptosis inhibitor. In this study, we investigate its underlying mechanism and find that while NAC primarily functions as a prodrug for cysteine, it may also directly counteract ferroptosis by serving as a reducing substrate for GPX4, the key regulator of ferroptosis. Furthermore, we demonstrate that GPX4 can utilize a wide range of reducing compounds, such as β-mercaptoethanol, as direct reducing substrates. This study enhances our understanding of NAC as a ferroptosis inhibitor and reveals that GPX4 may employ alternative reducing substrates to mitigate ferroptosis, particularly under glutathione-deficient conditions—an important consideration for future research.

SUMMARY

N-acetyl-L-cysteine (NAC) is a medication and a widely used antioxidant in cell death research. Despite its somewhat obscure mechanism of action, its role in inhibiting ferroptosis is gaining increasing recognition. In this study, we demonstrate that NAC treatment rapidly replenishes the intracellular cysteine pool, reinforcing its function as a prodrug for cysteine. Interestingly, its enantiomer, *N*-acetyl-D-cysteine (D-NAC), which cannot be converted into cysteine, also exhibits a strong anti-ferroptotic effect. We further clarify that NAC, D-NAC, and cysteine all act as direct reducing substrates for GPX4, counteracting lipid peroxidation. Consequently, only GPX4—rather than system x_c^-, glutathione biosynthesis, or ferroptosis suppressor protein 1—is necessary for NAC and D-NAC to prevent ferroptosis. Additionally, we identify a broad range of reducing substrates for GPX4 *in vitro*, including β-mercaptoethanol. These findings provide new insights into the mechanisms underlying the protective effects of NAC and other potential GPX4-reducing substrates against ferroptosis.

INTRODUCTION

N-acetyl-L-cysteine (NAC), an acetylated derivative of the amino acid L-cysteine, is used in the treatment of various pathological conditions, including autoimmune diseases, metabolic disorders, and neurological and psychiatric disorders, while its mechanism of action remains incompletely understood.[1] Traditionally, the biological effects of NAC were attributed to its roles in disulfide reduction and oxidant scavenging, but these assumptions have recently been questioned from a reaction kinetics perspective.[2] In contrast, the concept of NAC functioning as a pro-drug of cysteine, thereby exerting anti-ferroptotic effects, is being increasingly acknowledged.[3]

Ferroptosis is a unique form of cell death driven by iron-dependent lipid peroxidation downstream of metabolic dysfunction.[4] Ferroptosis has been implicated in a variety of diseases, such as ischemia-reperfusion injury, neurodegeneration, and autoimmune disorders, making its inhibition a promising therapeutic

Please cite this article in press as: Zheng et al., *N*-acetyl-L-cysteine averts ferroptosis by fostering glutathione peroxidase 4, Cell Chemical Biology (2025), https://doi.org/10.1016/j.chembiol.2025.04.002

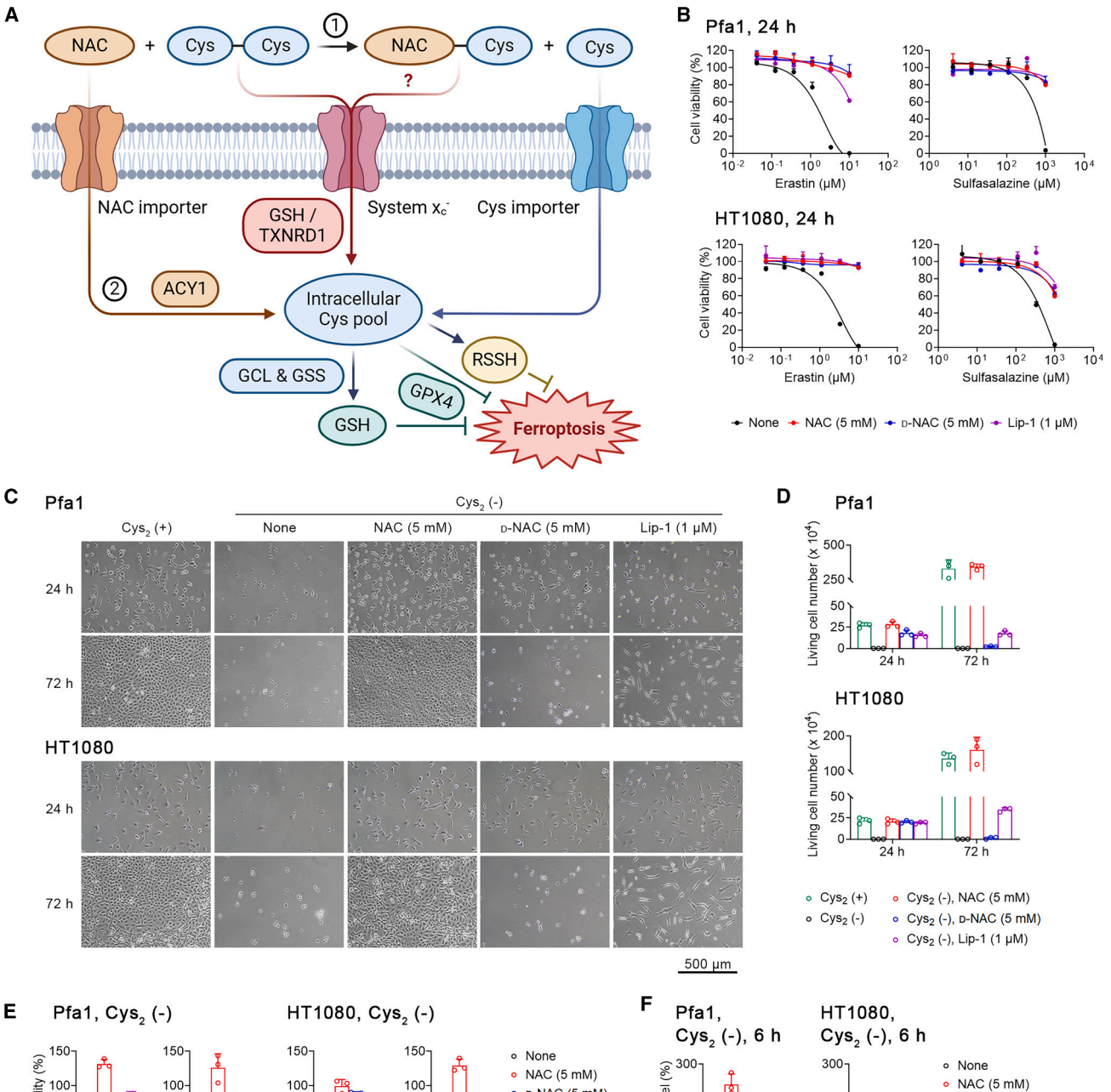

Figure 1. *N*-acetyl-D-cysteine protects cells cultured in cystine-free media from ferroptosis

(A) Schematic representation of the current understanding regarding the mechanism by which *N*-acetyl-L-cysteine (NAC) functions as a ferroptosis inhibitor. Cys, cysteine; GSH, glutathione; TXNRD1, thioredoxin reductase 1; ACY1, aminoacylase 1; GCL, glutamate cysteine ligase; GSS, glutathione synthetase; GPX4, glutathione peroxidase 4; RSSH, hydropersulfide.

(B) Cell viability of wild-type (WT) Pfa1 and HT1080 cells treated with the indicated concentrations of erastin and sulfasalazine in the presence or absence of 5 mM NAC, *N*-acetyl-D-cysteine (D-NAC), or 1 μM liproxstatin-1 (Lip-1) for 24 h.

(C) Cell morphology of WT Pfa1 and HT1080 cells cultured in normal media [Cys_2 (+)] or cystine-free [Cys_2 (-)] media in the presence or absence of 5 mM NAC, D-NAC, or 1 μM Lip-1 for 24 or 72 h.

(D) Number of living Pfa1 and HT1080 cells treated as described in (C). Dead cells were excluded by trypan blue staining.

(legend continued on next page)

Please cite this article in press as: Zheng et al., *N*-acetyl-L-cysteine averts ferroptosis by fostering glutathione peroxidase 4, Cell Chemical Biology (2025), https://doi.org/10.1016/j.chembiol.2025.04.002

strategy.[5] Ferroptosis induction typically involves disrupting the cysteine/glutathione (GSH)/glutathione peroxidase 4 (GPX4) axis. In cell culture, the main source of intracellular cysteine is extracellular cystine (an oxidized dimeric form of cysteine), which is imported via the cystine/glutamate antiporter system x_c^- and rapidly reduced to cysteine by the GSH or thioredoxin reductase 1 (TXNRD1) reducing systems (Figure 1A).[6]

In the presence of NAC, the intracellular cysteine pool can be replenished via two pathways. First, NAC may interact with extracellular cystine via disulfide exchange, releasing cysteine that then enters the cell via neutral amino acid transporters. Second, NAC can be imported into cells and directly converted to cysteine through aminoacylase 1 (ACY1)-mediated deacetylation (Figure 1A).[2]

Intracellular cysteine is required for GSH biosynthesis, a two-step enzymatic process catalyzed by glutamate cysteine ligase (GCL, aka γ-glutamylcysteine synthetase, γ-GCS) and GSH synthetase (GSS). GSH is subsequently utilized by GPX4 to reduce potentially detrimental (phospho)lipid hydroperoxides to their corresponding alcohols, thereby preventing ferroptosis (Figure 1A). In the absence of GSH, intracellular cysteine can serve as an alternative reducing substrate for GPX4, albeit with lower efficiency.[7,8] Additionally, intracellular cysteine can be used to generate hydrogen sulfide and sulfane sulfur species,[9] including hydropersulfides (RSSH), which are potential radical-trapping antioxidants that can inhibit ferroptosis in a GPX4-independent manner (Figure 1A).[10,11] In this study, we provide evidence that NAC inhibits ferroptosis by rapidly replenishing the intracellular cysteine pool. Furthermore, NAC and its enantiomer, *N*-acetyl-D-cysteine (D-NAC), may act as direct reducing substrates for GPX4, its expression being essential for NAC and D-NAC to counteract ferroptosis.

RESULTS AND DISCUSSION

D-NAC protects cells cultured in cystine-free media from ferroptosis

To investigate how NAC inhibits ferroptosis, we took advantage of its enantiomer D-NAC which cannot be deacetylated to cysteine.[2] Ferroptosis was induced in wild-type (WT) mouse fibroblast Pfa1 cells and human fibrosarcoma HT1080 cells via the treatment of increasing concentrations of erastin and sulfasalazine, *bona fide* inhibitors of system x_c^-.[12] We found that both NAC and D-NAC prevented the cell death, similar to the ferroptosis inhibitor liproxstatin-1 (Lip-1) (Figure 1B). These results are not surprising because D-NAC retains the ability to release cysteine from extracellular cystine, thus replenishing the intracellular cysteine pool independent of system x_c^- (Figure 1A). Surprisingly, however, D-NAC also prevented cell death in Pfa1 and HT1080 cells cultured in cystine-free medium, at least for 24 h (Figures 1C–1E). In this context, there should be no extracellular cystine that could form cysteine via disulfide exchange with D-NAC. In support of this, the intracellular cysteine level was not replenished by D-NAC or Lip-1 treatment upon cystine depletion, while NAC treatment robustly boosted the intracellular cysteine level within 6 h in both cell lines (Figure 1F). At 72 h after cystine depletion, only NAC but neither D-NAC nor Lip-1 could maintain the cell viability (Figures 1C–1E), indicating that the loss of cell viability occurring at 72 h is largely due to impaired cell proliferation or non-ferroptotic cell death.

To determine the role of system x_c^-, which is made up of the light chain xCT (encoded by *Slc7a11*) and the heavy chain 4F2,[13] we repeated these experiments with *Slc7a11* knockout (*Slc7a11*^{KO}) Pfa1 cells (Figure S1A) and *SLC7A11*^{KO} HT1080 cells.[12] These cell lines were maintained with β-mercaptoethanol (β-ME) to supply cysteine bypassing system x_c^-, as they would die otherwise.[14] After removing β-ME, cell death was largely prevented by NAC, D-NAC, and Lip-1 at 24 h, regardless of the presence or absence of extracellular cystine (Figures S1B and S1C). These findings suggest that the anti-ferroptotic effect of D-NAC is neither dependent on extracellular cystine nor on system x_c^-. At 72 h after β-ME removal, however, only NAC could sustain cell viability in both normal media and cystine-free media, while D-NAC only rescued cells cultured in normal media (Figures S1B and S1C). These results are consistent with the fact that NAC itself can be converted to cysteine, while D-NAC relies on extracellular cystine to replenish the intracellular cysteine pool.

To rule out potential residual cystine effects during the switch to cystine-free media, we intended to deplete cystine from the very beginning. To this end, cells were cultured in cystine-free media supplemented with cystathionine, which can serve as an alternative cysteine source through system x_c^--mediated uptake and cystathionine γ-lyase (CTH)-mediated hydrolysis (Figure S2A).[15] Notably, cystathionine cannot interact with NAC or D-NAC as it lacks a disulfide bond. Under these conditions, Pfa1 cells were able to proliferate, albeit more slowly, whereas HT1080 cells succumbed to death within 24 h (Figures S2B and S2C). A possible explanation for this discrepancy might be the higher expression of CTH and xCT in Pfa1 cells than HT1080 cells (Figures S2D and S2E). However, we were unable to directly compare xCT protein level due to the absence of a bifunctional antibody that detects both human and mouse xCT. Consistent with our previous results (Figures 1C–1E), NAC, D-NAC, and Lip-1 largely rescued Pfa1 cells challenged with erastin and sulfasalazine in cystine-free media supplemented with cystathionine (Figure S2F). These results confirm that extracellular cystine is indeed dispensable for the rescuing effects of NAC and D-NAC.

D-NAC counteracts ferroptosis in cystine-free media independently of GSH synthesis

We next explored whether GSH is involved in the anti-ferroptotic effect of D-NAC in cystine-free media. WT Pfa1 and HT1080 cells were treated with increasing concentrations of L-buthionine sulfoximine (BSO), a specific inhibitor of GCL required for GSH biosynthesis. In both cell lines, high concentrations of BSO caused the death of half the cells after 24 h, whereas NAC, D-NAC, and Lip-1 fully rescued the cells (Figure 2A). By contrast,

(E) Cell viability of Pfa1 and HT1080 cells treated as described in (C). Cells cultured in Cys_2 (+) media were used for normalization.
(F) Intracellular cysteine level of WT Pfa1 and HT1080 cells cultured in Cys_2 (-) media in the presence or absence of 5 mM NAC, D-NAC, or 1 μM Lip-1 for 6 h. Cells cultured in Cys_2 (+) media were used for normalization.
For (B), (D), (E), and (F), data are presented as mean + SD of $n = 3$ wells from one representative of two independent experiments.

Please cite this article in press as: Zheng et al., *N*-acetyl-L-cysteine averts ferroptosis by fostering glutathione peroxidase 4, Cell Chemical Biology (2025), https://doi.org/10.1016/j.chembiol.2025.04.002

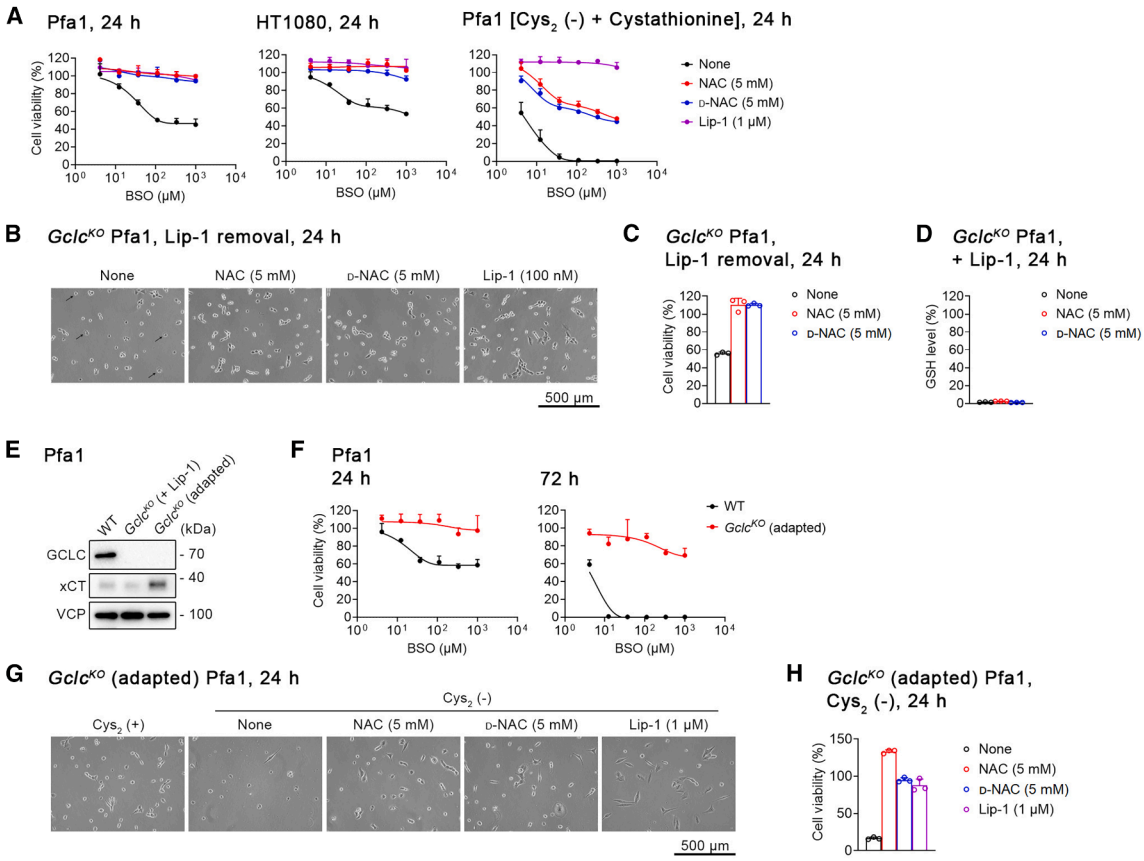

Figure 2. The anti-ferroptotic effect of D-NAC in cystine-free media is independent of GSH synthesis

(A) Cell viability of WT Pfa1 and HT1080 cells maintained in normal media, and Pfa1 cells maintained in Cys_2 (-) media supplemented with 200 μM cystathionine treated with the indicated concentrations of L-buthionine sulfoximine (BSO) in the presence or absence of 5 mM NAC, D-NAC, or 1 μM Lip-1 for 24 h.

(B) Cell morphology of GCL catalytic subunit knockout (*Gclc*^{KO}) Pfa1 cells cultured in the presence or absence of 5 mM NAC, D-NAC, or 100 nM Lip-1 for 24 h.

(C) Cell viability of *Gclc*^{KO} Pfa1 cells treated as described in (B). *Gclc*^{KO} cells without Lip-1 removal were used for normalization.

(D) Intracellular GSH level of *Gclc*^{KO} Pfa1 cells cultured in the presence or absence of 5 mM NAC or D-NAC for 24 h. The cells were supplemented with 100 nM Lip-1 to prevent cell death. WT cells were used for normalization.

(E) Immunoblots of GCLC and xCT in WT, *Gclc*^{KO} (supplemented with 1 μM Lip-1), and *Gclc*^{KO} (adapted) Pfa1 cells. Valosin-containing protein (VCP) is the loading control.

(F) Cell viability of WT and *Gclc*^{KO} (adapted) Pfa1 cells treated with the indicated concentrations of BSO for 24 or 72 h.

(G) Cell morphology of *Gclc*^{KO} (adapted) Pfa1 cells cultured in Cys_2 (+) or Cys_2 (-) media in the presence or absence of 5 mM NAC, D-NAC, or 1 μM Lip-1, for 24 h.

(H) Cell viability of *Gclc*^{KO} (adapted) Pfa1 cells treated as described in (G). Cells cultured in Cys_2 (+) media were used for normalization.

For (A), (C), (D), (F), and (H), data are presented as mean + SD of $n = 3$ wells from one representative of two independent experiments.

Pfa1 cells cultured in cystine-free media supplemented with cystathionine were much more sensitive to BSO (Figure 2A), likely due to their limited levels of intracellular cysteine and GSH. In this context, NAC and D-NAC robustly prevented death in half of the cells (Figure 2A), suggesting that the anti-ferroptotic effect of D-NAC does not rely on GSH biosynthesis.

To further test this hypothesis, we generated Pfa1 cells with targeted deletion of *Gclc*. These cells require Lip-1 for survival, as otherwise they would die of ferroptosis. When Lip-1 was removed, half of the cells died within 24 h, while NAC and D-NAC fully rescued them (Figures 2B and 2C). We further confirmed that treatment with NAC and D-NAC did not restore GSH level in *Gclc*^{KO} cells (Figure 2D). *Gclc*-deficient mouse embryonic fibroblasts are known to survive with NAC or forced xCT expression.[6,16] We therefore adapted *Gclc*^{KO} Pfa1 cells by gradually reducing Lip-1 concentration, enabling them to proliferate infinitely in the absence of Lip-1. The loss of GCLC was validated by immunoblotting, and an upregulation of xCT was observed in adapted *Gclc*^{KO} cells (Figure 2E). As expected, these cells were fully resistant to BSO (Figure 2F) but still dependent on cystine uptake for survival (Figures 2G and 2H). In cystine-free conditions, NAC, D-NAC, and Lip-1 largely prevented cell death at 24 h (Figures 2G and 2H), confirming that the anti-ferroptotic effect of D-NAC in cystine-free media is independent of GSH.

NAC and D-NAC counteract ferroptosis in a GPX4-dependent manner

To clarify how D-NAC prevents ferroptosis in cystine-free media, we investigated the role of GPX4. WT Pfa1 and HT1080 cells were treated with increasing concentrations of a series of GPX4 inhibitors, including *(1S,3R)*-RSL3 (RSL3), ML162, ML210, FIN56, and $FINO_2$. In both cell lines, the cell death

Please cite this article in press as: Zheng et al., *N*-acetyl-L-cysteine averts ferroptosis by fostering glutathione peroxidase 4, Cell Chemical Biology (2025), https://doi.org/10.1016/j.chembiol.2025.04.002

CellPress
OPEN ACCESS

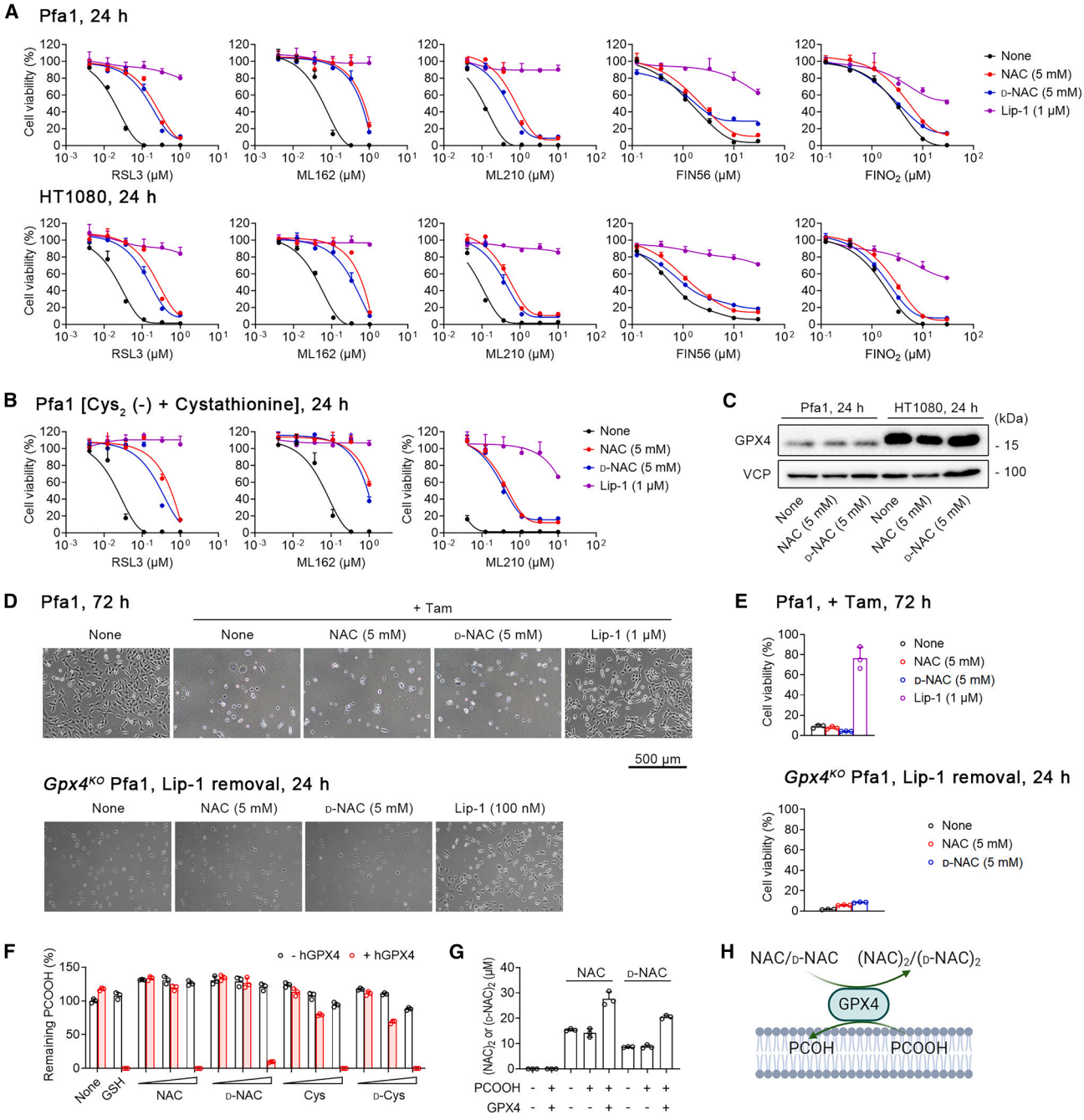

Figure 3. The anti-ferroptotic effects of NAC and D-NAC rely on the presence of GPX4

(A) Cell viability of WT Pfa1 and HT1080 cells treated with the indicated concentrations of (1*S*,3*R*)-RSL3 (RSL3), ML162, ML210, FIN56, and $FINO_2$ in the presence or absence of 5 mM NAC, D-NAC, or 1 μM Lip-1 for 24 h.

(B) Cell viability of WT Pfa1 cells maintained in Cys_2 (-) media supplemented with 200 μM cystathionine and treated with the indicated concentrations of RSL3, ML162, and ML210 in the presence or absence of 5 mM NAC, D-NAC, or 1 μM Lip-1 for 24 h.

(C) Immunoblot analysis of GPX4 in WT Pfa1 cells and HT1080 cells cultured in the presence or absence of 5 mM NAC or D-NAC for 24 h. VCP was used as loading control.

(D) Cell morphology of WT Pfa1 cells treated with or without (*Z*)-4-hydroxytamoxifen (Tam) in the presence or absence of 5 mM NAC, D-NAC, or 1 μM Lip-1 for 72 h (upper panels), and glutathione peroxidase 4 knockout (*Gpx4*^{KO}) Pfa1 cells cultured in the presence or absence of 5 mM NAC, D-NAC, or 100 nM Lip-1 (lower panels).

(E) Cell viability of WT and *Gpx4*^{KO} Pfa1 cells treated as described in (D). WT cells without Tam treatment and *Gpx4*^{KO} cells without Lip-1 removal were used for normalization, respectively.

(legend continued on next page)

Please cite this article in press as: Zheng et al., *N*-acetyl-L-cysteine averts ferroptosis by fostering glutathione peroxidase 4, Cell Chemical Biology (2025), https://doi.org/10.1016/j.chembiol.2025.04.002

induced by RSL3, ML162, and ML210 within a specific concentration range could largely be rescued by NAC and D-NAC, whereas the cell death induced by FIN56 and $FINO_2$ was barely affected by NAC and D-NAC treatment (Figure 3A). This discrepancy might be due to the distinct mechanisms of action of these inhibitors. While RSL3, ML162, and ML210 covalently inhibit GPX4 by binding to its active site selenocysteine, FIN56 and $FINO_2$ act by promoting GPX4 degradation and indirectly inhibiting GPX4's enzymatic function.[17] Furthermore, FIN56 and $FINO_2$ may induce ferroptosis via GPX4-independent mechanisms.[18,19]

Since NAC and D-NAC only showed rescue effects on RSL3, ML162, and ML210-induced ferroptosis (Figure 3A), we further challenged Pfa1 cells cultured in cystine-free media supplemented with cystathionine with these ferroptosis inducers, yielding consistent results (Figure 3B). Notably, the rescue effects of NAC and D-NAC diminished when cells were exposed to high concentrations of RSL3, ML162, and ML210, whereas cells remained fully viable in the presence of Lip-1, ruling out non-ferroptotic cell death (Figures 3A and 3B). This suggests that NAC and D-NAC are unable to rescue ferroptosis when GPX4 is completely inhibited.

We then asked whether NAC and D-NAC treatment might increase GPX4 expression and thereby confer ferroptosis resistance. However, this possibility was ruled out in both Pfa1 and HT1080 cell lines (Figure 3C). GPX4 inhibitors, such as RSL3, are known to have off-target effects on other selenoproteins.[20,21] To validate the role of GPX4, we used a genetic approach to perturb its expression. In Pfa1 cells, *Gpx4* can be genetically ablated by 4-hydroxytamoxifen (Tam) treatment.[22] After Tam treatment, only Lip-1, and not NAC or D-NAC, rescued cell death (Figures 3D and 3E). We further tested $Gpx4^{KO}$ Pfa1 cells, which were maintained in the presence of Lip-1.[23] Consistently, neither NAC nor D-NAC rescued cell death upon Lip-1 removal (Figures 3D and 3E), indicating that the presence of GPX4 is a prerequisite for NAC and D-NAC to counteract ferroptosis.

Given that cysteine has been reported to act as a reducing substrate of GPX4,[7,8] we wondered whether NAC and D-NAC could act similarly. Using an *in vitro* GPX4 enzymatic activity assay as recently reported by us,[23] we demonstrated that GPX4 could fully reduce phosphatidylcholine hydroperoxide (PCOOH) in the presence of 1 mM NAC, D-NAC, cysteine, or D-cysteine (Figure 3F), suggesting that NAC and D-NAC are *bona fide* reducing substrates of GPX4. Accordingly, the oxidized products of NAC and D-NAC, i.e., *N*,*N*′-diacetyl-L-cystine [$(NAC)_2$] and *N*,*N*′-diacetyl-D-cystine [$(D\text{-}NAC)_2$], respectively, were detectable (Figure 3G). Although NAC and D-NAC compounds *per se* contain ~1% $(NAC)_2$ or $(D\text{-}NAC)_2$, their concentrations increased by ~10 μM in the presence of PCOOH and GPX4, corresponding to the concentration of PCOOH (Figure 3G). As such, we propose that two molecules of NAC or D-NAC are oxidized by GPX4 to form one molecule of $(NAC)_2$ or $(D\text{-}NAC)_2$, thereby forming a disulfide bond and donating two hydrogen atoms (Figure 3H).

Ferroptosis suppressor protein 1 (FSP1) is the second mainstay in ferroptosis that prevents lipid peroxidation and ferroptosis independent of GPX4. Unlike the cysteine/GSH/GPX4 axis, FSP1 halts lipid peroxidation by reducing coenzyme Q or vitamin K, which in turn react with lipid peroxyl radicals.[24–26] To explore whether FSP1 might be involved in the anti-ferroptotic effects of NAC and D-NAC, we took advantage of the $Gpx4^{KO}$ Pfa1 cells overexpressing human FSP1. As expected, these cells were resistant to cystine depletion- and BSO treatment-induced ferroptosis, although they proliferated more slowly in cystine-free media (Figures S3A and S3B). We then challenged these cells with a panel of FSP1 inhibitors, including iFSP1,[25] icFSP1,[27] viFSP1,[28] and WIN 62,577.[23] In these conditions, NAC and D-NAC only displayed minimal rescuing effects (Figure S3C). Similar findings were obtained with $GPX4^{KO}$ $hFSP1^{OE}$ HT1080 cells (Figures S3D–S3F). By contrast, NAC and D-NAC largely rescued $FSP1^{KO}$ HT1080 cells upon treatment with the GPX4 inhibitors RSL3, ML162, and ML210 (Figure S3G). These results thus confirm that GPX4, rather than FSP1, is required for NAC and D-NAC to exert anti-ferroptotic effects.

The anti-ferroptotic effects of xCT overexpression and β-ME rely on GPX4

Since NAC is a pro-drug of cysteine while cysteine was proposed to inhibit ferroptosis independently of GPX4 (Figure 1A), we were puzzled by the finding that the anti-ferroptotic effects of both NAC and D-NAC strictly relied on GPX4. Notably, a previous study suggested that Pfa1 cells overexpressing xCT were resistant to GPX4 deficiency-induced ferroptosis due to increased cysteine availability.[11] To explore this, we repeated the experiment and generated a similar cell line in our lab. As expected, Pfa1 cells overexpressing mouse xCT ($mSlc7a11^{OE}$) were significantly more resistant to erastin and sulfasalazine compared to the parental cells (Figure S4A). Furthermore, $mSlc7a11^{OE}$ cells exhibited greater resistance to BSO, RSL3, and ML210 than WT control cells (Figure S4A). Interestingly, at higher concentrations of RSL3 and ML210, $mSlc7a11^{OE}$ cells succumbed to ferroptosis, which was fully counteracted by Lip-1 treatment (Figure S4A), mimicking the effects observed with NAC and D-NAC (Figure 3A).

We then treated $mSlc7a11^{OE}$ cells with Tam to delete *Gpx4* gene. To our surprise, $mSlc7a11^{OE}$ cells showed no difference from WT cells at 72 h after Tam treatment, i.e., both cell lines were completely dead (Figures S4B and S4C). The discrepancy between our observations and the previous report might be due to the higher dose of Tam (1 μM instead of 0.5 μM) we used, which resulted in a faster GPX4 ablation.[11] Indeed, at an earlier time point (i.e., 48 h) xCT overexpression did have protective

(F) Relative amount of remaining phosphatidylcholine hydroperoxide (PCOOH) analyzed by LC-MS/MS after incubation with or without affinity-purified human GPX4 (hGPX4) in the presence or absence of GSH (1 mM), NAC (10 μM, 100 μM, 1 mM), D-NAC (10 μM, 100 μM, 1 mM), Cys (10 μM, 100 μM, 1 mM), and D-Cys (10 μM, 100 μM, 1 mM) for 1 h at 37°C. Data represent the intensity of PCOOH.

(G) Concentrations of $(NAC)_2$ or $(D\text{-}NAC)_2$ analyzed by LC-MS/MS after incubation with or without affinity-purified hGPX4 and 10 μM PCOOH, in the presence or absence of 1 mM NAC and D-NAC for 1 h at 37°C.

(H) Schematic representation of the mechanism by which GPX4 reduces PCOOH using NAC or D-NAC as reducing substrates.

For (A), (B), (E), (F), and (G), data are presented as mean + SD of $n = 3$ wells from one representative of two independent experiments.

Please cite this article in press as: Zheng et al., *N*-acetyl-L-cysteine averts ferroptosis by fostering glutathione peroxidase 4, Cell Chemical Biology (2025), https://doi.org/10.1016/j.chembiol.2025.04.002

CellPress
OPEN ACCESS

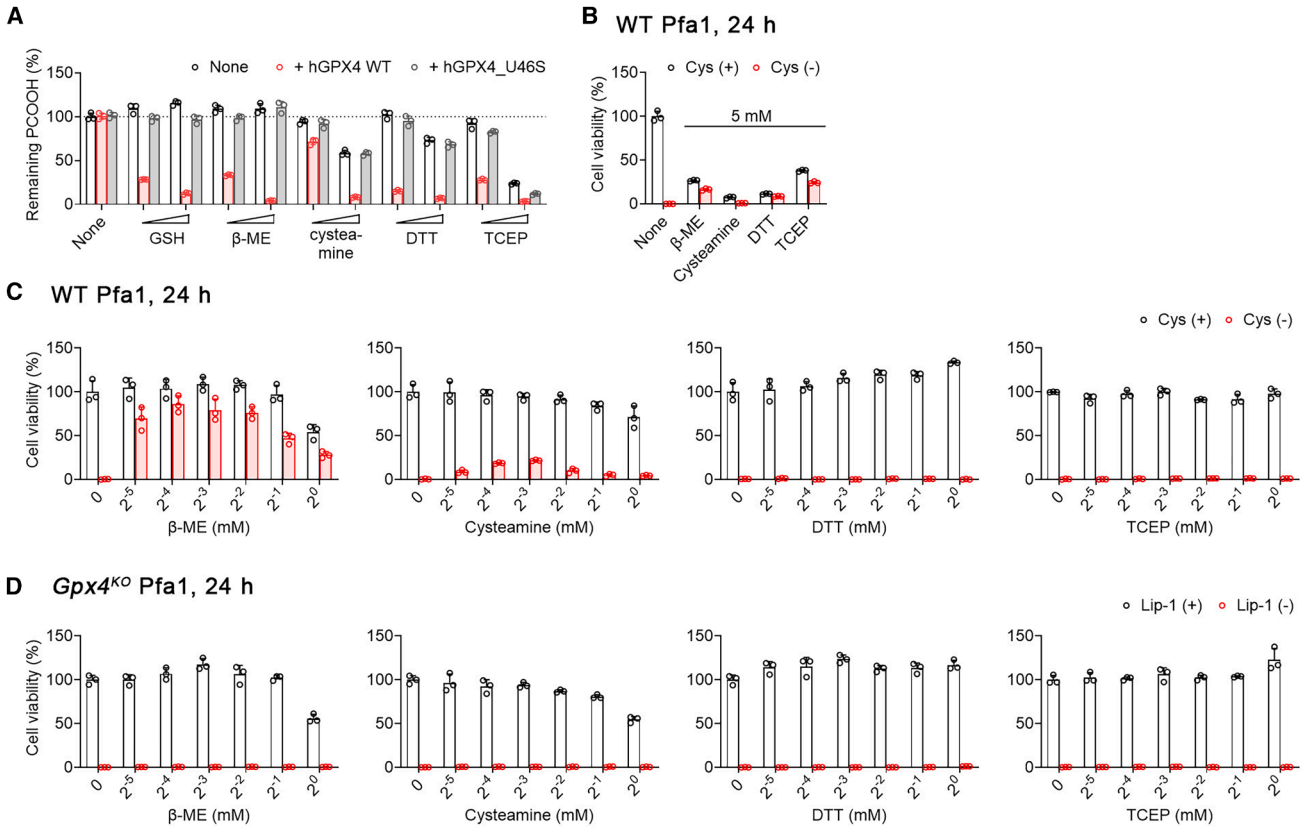

Figure 4. β-mercaptoethanol is a reducing substrate of GPX4 and its anti-ferroptotic effect relies on the presence of GPX4

(A) Relative amount of remaining PCOOH analyzed by LC-MS/MS after incubation with or without affinity-purified hGPX4_WT or hGPX4_U46S in the presence or absence of GSH, β-mercaptoethanol (β-ME), cysteamine, dithiothreitol (DTT), and tris(2-carboxyethyl)phosphine (TCEP) at 100 μM or 1 mM concentrations for 1 h at 37°C. Data represent the intensity of PCOOH.

(B) Cell viability of WT Pfa1 cells cultured in Cys_2 (+) or Cys_2 (-) media in the presence or absence of 5 mM β-ME, cysteamine, DTT, and TCEP for 24 h.

(C) Cell viability of WT Pfa1 cells cultured in Cys_2 (+) or Cys_2 (-) media in the presence or absence of the indicated concentrations of β-ME, cysteamine, DTT, and TCEP for 24 h.

(D) Cell viability of *Gpx4*^{KO} Pfa1 cells cultured in the presence or absence of 100 nM Lip-1 and treated with the indicated concentrations of β-ME, cysteamine, DTT and TCEP for 24 h.

For all the panels, data are presented as mean + SD of $n = 3$ wells from one representative of two independent experiments.

effects as we previously reported.[29] To further corroborate these results, two single cell clones of *mSlc7a11*^{OE} *Gpx4*^{KO} Pfa1 were generated. When cultured in the absence of Lip-1, both clones died (Figures S4B and S4C). The overexpression of xCT and the loss of GPX4 were confirmed by immunoblotting (Figure S4D). These results thus suggest that the anti-ferroptotic effect of xCT overexpression depends on the presence of GPX4.

Another confounding finding was that β-ME rescued *Slc7a11*^{KO} Pfa1 cells and *SLC7A11*^{KO} HT1080 cells in cystine-free media at 24 h (Figures S1B and S1C). Theoretically, β-ME functions as a cystine shuttle similar to NAC (Figure 1A), although it cannot be converted to cysteine. However, the protective effect of β-ME in cystine-free media prompted us to speculate whether β-ME could also serve as a reducing substrate for GPX4. To test this, we conducted an *in vitro* GPX4 enzymatic activity assay, which revealed that β-ME, along with other reducing agents like cysteamine, dithiothreitol (DTT) and tris(2-carboxyethyl)phosphine (TCEP), could act as reducing substrates for GPX4 (Figure 4A). Notably, cysteamine, DTT and especially TCEP were able to directly reduce PCOOH in the absence of GPX4 (Figure 4A). However, these agents were significantly more cytotoxic than NAC and D-NAC and could not be used at a 5 mM concentration in cell experiments (Figure 4B). At lower concentrations, only β-ME exhibited a strong protective effect against cystine depletion-induced cell death (Figure 4C), while none of these agents could rescue *Gpx4*^{KO} Pfa1 cells from Lip-1 removal (Figure 4D). The failure of cysteamine, DTT and TCEP to rescue cells from cystine depletion-induced ferroptosis may be due to differences in their subcellular localization, stability, and cell permeability.

In summary, the findings from this study unambiguously demonstrate that NAC and D-NAC are *bona fide* reducing substrates of GPX4. However, since NAC is rapidly converted to cysteine (Figure 1F) and GSH is the preferred substrate for GPX4, the anti-ferroptotic effect of NAC is likely primarily due to its role in replenishing the intracellular GSH pool. Nevertheless, when GSH biosynthesis is blocked or GSH is depleted, for instance in response to drug conjugation, NAC and its

metabolite cysteine may still serve as direct reducing substrates for GPX4 due to its promiscuity toward both the reducing and oxidizing substrates.[30] This notion is supported by earlier findings that oral NAC supplementation rescued lethality of hepatocyte-specific *Gclc* knockout mice.[31] Moreover, our data implicate a broad range of commonly used reducing substrates for GPX4, at least in cell-free systems. Thus, our results not only deepen our understanding of the mechanism of action of NAC in cell protection, but also provide valuable insights for the field of ferroptosis research.

Limitations of the study

These findings are based on experiments conducted with a limited set of cell lines and *in vitro* enzymatic assays. Further investigation is needed to determine the potential of NAC and D-NAC to act as direct reducing substrates for GPX4 under physiological conditions. However, this possibility is highly likely, considering that NAC is used to treat various pathological conditions in humans and has demonstrated the ability to rescue transgenic mice from lethality caused by liver-specific GSH depletion.

RESOURCE AVAILABILITY

Lead contact

Further information and requests for resources and reagents should be directed to and will be fulfilled by the lead contact, Marcus Conrad (marcus.conrad@helmholtz-munich.de).

Materials availability

All reagents and materials are listed in the key resources table. Materials are available on reasonable request.

Data and code availability

- All data reported in this paper will be shared by the lead contact upon request.
- This paper does not report original code.
- Any additional information required to reanalyze the data reported in this paper is available from the lead contact upon request.

ACKNOWLEDGMENTS

We thank Dr. Toshitaka Nakamura (Helmholtz Munich) for helping with the generation of plasmids. This work was supported by the Deutsche Forschungsgemeinschaft (CO 291/7-1), the DFG Priority Program SPP 2306 [CO 291/9-1, #461385412; CO 291/10-1, #461507177; CO 291/9-2, CO 291/10-2, CO 291/14-1] and the CRC TRR 353 (CO 291/11-1; #471011418), the German Federal Ministry of Education and Research (01EJ2205B), and the European Research Council under the European Union's Horizon 2020 research and innovation programme (grant agreement no. GA 884754) to M.C. W.Z. and C.X. are supported by China Scholarship Council. All the schematic illustrations were created with BioRender.com.

AUTHOR CONTRIBUTIONS

J.Z., W.Z., and M.C. conceived experiments; J.Z., W.Z., J.I., B.H., and C.X. conducted experiments; E.M. provided expert feedback; J.Z. wrote the manuscript, revised by E.M. and M.C.

DECLARATION OF INTERESTS

M.C. is a co-founder and shareholder of ROSCUE Therapeutics GmbH and holds patents for some of the compounds described herein.

STAR★METHODS

Detailed methods are provided in the online version of this paper and include the following:

- KEY RESOURCES TABLE
- EXPERIMENTAL MODEL AND STUDY PARTICIPANT DETAILS
  - Cell lines
- METHOD DETAILS
  - Reagents
  - Generation of knockout cell lines
  - Overexpression of xCT by viral transduction
  - qPCR analysis
  - Immunoblotting
  - Cell viability
  - Cell morphology
  - Living cell counting
  - GPX4 activity assay
  - LC-MS/MS
- QUANTIFICATION AND STATISTICAL ANALYSIS

SUPPLEMENTAL INFORMATION

Supplemental information can be found online at https://doi.org/10.1016/j.chembiol.2025.04.002.

Received: October 2, 2024
Revised: March 8, 2025
Accepted: April 9, 2025
Published: April 30, 2025

REFERENCES

1. Schwalfenberg, G.K. (2021). N-Acetylcysteine: A Review of Clinical Usefulness (an Old Drug with New Tricks). J. Nutr. Metab. *2021*, 9949453. https://doi.org/10.1155/2021/9949453.
2. Pedre, B., Barayeu, U., Ezeriņa, D., and Dick, T.P. (2021). The mechanism of action of N-acetylcysteine (NAC): The emerging role of H2S and sulfane sulfur species. Pharmacol. Ther. *228*, 107916. https://doi.org/10.1016/j.pharmthera.2021.107916.
3. Kalyanaraman, B. (2022). NAC, NAC, Knockin' on Heaven's door: Interpreting the mechanism of action of N-acetylcysteine in tumor and immune cells. Redox Biol. *57*, 102497. https://doi.org/10.1016/j.redox.2022.102497.
4. Zheng, J., and Conrad, M. (2020). The Metabolic Underpinnings of Ferroptosis. Cell Metab. *32*, 920–937. https://doi.org/10.1016/j.cmet.2020.10.011.
5. Zheng, J., and Conrad, M. (2025). Ferroptosis: when metabolism meets cell death. Physiol. Rev. *105*, 651–706. https://doi.org/10.1152/physrev.00031.2024.
6. Mandal, P.K., Seiler, A., Perisic, T., Kölle, P., Banjac Canak, A., Förster, H., Weiss, N., Kremmer, E., Lieberman, M.W., Bannai, S., et al. (2010). System x(c)- and thioredoxin reductase 1 cooperatively rescue glutathione deficiency. J. Biol. Chem. *285*, 22244–22253. https://doi.org/10.1074/jbc.M110.121327.
7. Roveri, A., Maiorino, M., Nisii, C., and Ursini, F. (1994). Purification and characterization of phospholipid hydroperoxide glutathione peroxidase from rat testis mitochondrial membranes. Biochim. Biophys. Acta *1208*, 211–221. https://doi.org/10.1016/0167-4838(94)90106-6.
8. Xia, C., Xing, X., Zhang, W., Wang, Y., Jin, X., Wang, Y., Tian, M., Ba, X., and Hao, F. (2024). Cysteine and homocysteine can be exploited by GPX4 in ferroptosis inhibition independent of GSH synthesis. Redox Biol. *69*, 102999. https://doi.org/10.1016/j.redox.2023.102999.
9. Ezerina, D., Takano, Y., Hanaoka, K., Urano, Y., and Dick, T.P. (2018). N-Acetyl Cysteine Functions as a Fast-Acting Antioxidant by Triggering

Intracellular H(2)S and Sulfane Sulfur Production. Cell Chem. Biol. *25*, 447–459.e444. https://doi.org/10.1016/j.chembiol.2018.01.011.

10. Wu, Z., Khodade, V.S., Chauvin, J.P.R., Rodriguez, D., Toscano, J.P., and Pratt, D.A. (2022). Hydropersulfides Inhibit Lipid Peroxidation and Protect Cells from Ferroptosis. J. Am. Chem. Soc. *144*, 15825–15837. https://doi.org/10.1021/jacs.2c06804.
11. Barayeu, U., Schilling, D., Eid, M., Xavier da Silva, T.N., Schlicker, L., Mitreska, N., Zapp, C., Gräter, F., Miller, A.K., Kappl, R., et al. (2023). Hydropersulfides inhibit lipid peroxidation and ferroptosis by scavenging radicals. Nat. Chem. Biol. *19*, 28–37. https://doi.org/10.1038/s41589-022-01145-w.
12. Zheng, J., Sato, M., Mishima, E., Sato, H., Proneth, B., and Conrad, M. (2021). Sorafenib fails to trigger ferroptosis across a wide range of cancer cell lines. Cell Death Dis. *12*, 698. https://doi.org/10.1038/s41419-021-03998-w.
13. Sato, H., Tamba, M., Ishii, T., and Bannai, S. (1999). Cloning and expression of a plasma membrane cystine/glutamate exchange transporter composed of two distinct proteins. J. Biol. Chem. *274*, 11455–11458. https://doi.org/10.1074/jbc.274.17.11455.
14. Sato, H., Shiiya, A., Kimata, M., Maebara, K., Tamba, M., Sakakura, Y., Makino, N., Sugiyama, F., Yagami, K.i., Moriguchi, T., et al. (2005). Redox imbalance in cystine/glutamate transporter-deficient mice. J. Biol. Chem. *280*, 37423–37429. https://doi.org/10.1074/jbc.M506439200.
15. Kobayashi, S., Sato, M., Kasakoshi, T., Tsutsui, T., Sugimoto, M., Osaki, M., Okada, F., Igarashi, K., Hiratake, J., Homma, T., et al. (2015). Cystathionine is a novel substrate of cystine/glutamate transporter: implications for immune function. J. Biol. Chem. *290*, 8778–8788. https://doi.org/10.1074/jbc.M114.625053.
16. Shi, Z.Z., Osei-Frimpong, J., Kala, G., Kala, S.V., Barrios, R.J., Habib, G. M., Lukin, D.J., Danney, C.M., Matzuk, M.M., and Lieberman, M.W. (2000). Glutathione synthesis is essential for mouse development but not for cell growth in culture. Proc. Natl. Acad. Sci. USA *97*, 5101–5106. https://doi.org/10.1073/pnas.97.10.5101.
17. Nakamura, T., and Conrad, M. (2024). Exploiting ferroptosis vulnerabilities in cancer. Nat. Cell Biol. *26*, 1407–1419. https://doi.org/10.1038/s41556-024-01425-8.
18. Shimada, K., Skouta, R., Kaplan, A., Yang, W.S., Hayano, M., Dixon, S.J., Brown, L.M., Valenzuela, C.A., Wolpaw, A.J., and Stockwell, B.R. (2016). Global survey of cell death mechanisms reveals metabolic regulation of ferroptosis. Nat. Chem. Biol. *12*, 497–503. https://doi.org/10.1038/nchembio.2079.
19. Gaschler, M.M., Andia, A.A., Liu, H., Csuka, J.M., Hurlocker, B., Vaiana, C. A., Heindel, D.W., Zuckerman, D.S., Bos, P.H., Reznik, E., et al. (2018). FINO2 initiates ferroptosis through GPX4 inactivation and iron oxidation. Nat. Chem. Biol. *14*, 507–515. https://doi.org/10.1038/s41589-018-0031-6.
20. Gao, J., Yang, F., Che, J., Han, Y., Wang, Y., Chen, N., Bak, D.W., Lai, S., Xie, X., Weerapana, E., and Wang, C. (2018). Selenium-Encoded Isotopic Signature Targeted Profiling. ACS Cent. Sci. *4*, 960–970. https://doi.org/10.1021/acscentsci.8b00112.
21. Eaton, J.K., Ruberto, R.A., Kramm, A., Viswanathan, V.S., and Schreiber, S.L. (2019). Diacylfuroxans Are Masked Nitrile Oxides That Inhibit GPX4 Covalently. J. Am. Chem. Soc. *141*, 20407–20415. https://doi.org/10.1021/jacs.9b10769.
22. Seiler, A., Schneider, M., Förster, H., Roth, S., Wirth, E.K., Culmsee, C., Plesnila, N., Kremmer, E., Rådmark, O., Wurst, W., et al. (2008). Glutathione peroxidase 4 senses and translates oxidative stress into 12/15-lipoxygenase dependent- and AIF-mediated cell death. Cell Metab. *8*, 237–248. https://doi.org/10.1016/j.cmet.2008.07.005.
23. Nakamura, T., Ito, J., Mourão, A.S.D., Wahida, A., Nakagawa, K., Mishima, E., and Conrad, M. (2024). A tangible method to assess native ferroptosis suppressor activity. Cell Rep. Methods *4*, 100710. https://doi.org/10.1016/j.crmeth.2024.100710.
24. Bersuker, K., Hendricks, J.M., Li, Z., Magtanong, L., Ford, B., Tang, P.H., Roberts, M.A., Tong, B., Maimone, T.J., Zoncu, R., et al. (2019). The CoQ oxidoreductase FSP1 acts parallel to GPX4 to inhibit ferroptosis. Nature *575*, 688–692. https://doi.org/10.1038/s41586-019-1705-2.
25. Doll, S., Freitas, F.P., Shah, R., Aldrovandi, M., da Silva, M.C., Ingold, I., Goya Grocin, A., Xavier da Silva, T.N., Panzilius, E., Scheel, C.H., et al. (2019). FSP1 is a glutathione-independent ferroptosis suppressor. Nature *575*, 693–698. https://doi.org/10.1038/s41586-019-1707-0.
26. Mishima, E., Ito, J., Wu, Z., Nakamura, T., Wahida, A., Doll, S., Tonnus, W., Nepachalovich, P., Eggenhofer, E., Aldrovandi, M., et al. (2022). A non-canonical vitamin K cycle is a potent ferroptosis suppressor. Nature *608*, 778–783. https://doi.org/10.1038/s41586-022-05022-3.
27. Nakamura, T., Hipp, C., Santos Dias Mourão, A., Borggräfe, J., Aldrovandi, M., Henkelmann, B., Wanninger, J., Mishima, E., Lytton, E., Emler, D., et al. (2023). Phase separation of FSP1 promotes ferroptosis. Nature *619*, 371–377. https://doi.org/10.1038/s41586-023-06255-6.
28. Nakamura, T., Mishima, E., Yamada, N., Mourão, A.S.D., Trümbach, D., Doll, S., Wanninger, J., Lytton, E., Sennhenn, P., Nishida Xavier da Silva, T., et al. (2023). Integrated chemical and genetic screens unveil FSP1 mechanisms of ferroptosis regulation. Nat. Struct. Mol. Biol. *30*, 1806–1815. https://doi.org/10.1038/s41594-023-01136-y.
29. Doll, S., Proneth, B., Tyurina, Y.Y., Panzilius, E., Kobayashi, S., Ingold, I., Irmler, M., Beckers, J., Aichler, M., Walch, A., et al. (2017). ACSL4 dictates ferroptosis sensitivity by shaping cellular lipid composition. Nat. Chem. Biol. *13*, 91–98. https://doi.org/10.1038/nchembio.2239.
30. Conrad, M., Schneider, M., Seiler, A., and Bornkamm, G.W. (2007). Physiological role of phospholipid hydroperoxide glutathione peroxidase in mammals. Biol. Chem. *388*, 1019–1025. https://doi.org/10.1515/BC.2007.130.
31. Chen, Y., Johansson, E., Yang, Y., Miller, M.L., Shen, D., Orlicky, D.J., Shertzer, H.G., Vasiliou, V., Nebert, D.W., and Dalton, T.P. (2010). Oral N-acetylcysteine rescues lethality of hepatocyte-specific Gclc-knockout mice, providing a model for hepatic cirrhosis. J. Hepatol. *53*, 1085–1094. https://doi.org/10.1016/j.jhep.2010.05.028.
32. Mishima, E., Nakamura, T., Zheng, J., Zhang, W., Mourão, A.S.D., Sennhenn, P., and Conrad, M. (2023). DHODH inhibitors sensitize to ferroptosis by FSP1 inhibition. Nature *619*, E9–E18. https://doi.org/10.1038/s41586-023-06269-0.
33. Stringer, B.W., Day, B.W., D'Souza, R.C.J., Jamieson, P.R., Ensbey, K.S., Bruce, Z.C., Lim, Y.C., Goasdoué, K., Offenhäuser, C., Akgül, S., et al. (2019). A reference collection of patient-derived cell line and xenograft models of proneural, classical and mesenchymal glioblastoma. Sci. Rep. *9*, 4902. https://doi.org/10.1038/s41598-019-41277-z.
34. Michlits, G., Jude, J., Hinterndorfer, M., de Almeida, M., Vainorius, G., Hubmann, M., Neumann, T., Schleiffer, A., Burkard, T.R., Fellner, M., et al. (2020). Multilayered VBC score predicts sgRNAs that efficiently generate loss-of-function alleles. Nat. Methods *17*, 708–716. https://doi.org/10.1038/s41592-020-0850-8.
35. Ito, J., Nakamura, T., Toyama, T., Chen, D., Berndt, C., Poschmann, G., Mourão, A.S.D., Doll, S., Suzuki, M., Zhang, W., et al. (2024). PRDX6 dictates ferroptosis sensitivity by directing cellular selenium utilization. Mol. Cell *84*, 4629–4644.e9. https://doi.org/10.1016/j.molcel.2024.10.028.
36. Ito, J., Nakagawa, K., Kato, S., Hirokawa, T., Kuwahara, S., Nagai, T., and Miyazawa, T. (2015). Direct separation of the diastereomers of phosphatidylcholine hydroperoxide bearing 13-hydroperoxy-9Z,11E-octadecadienoic acid using chiral stationary phase high-performance liquid chromatography. J. Chromatogr. A *1386*, 53–61. https://doi.org/10.1016/j.chroma.2015.01.080.

Please cite this article in press as: Zheng et al., *N*-acetyl-L-cysteine averts ferroptosis by fostering glutathione peroxidase 4, Cell Chemical Biology (2025), https://doi.org/10.1016/j.chembiol.2025.04.002

STAR★METHODS

KEY RESOURCES TABLE

REAGENT or RESOURCE	SOURCE	IDENTIFIER
Antibodies		
Rabbit polyclonal anti-γ-GCSc (1:200)	Santa Cruz	Cat#sc-22755; RRID: AB_675582
Rabbit polyclonal anti-CTH (1:1000)	GeneTex	Cat#GTX113409; RRID: AB_2038238
Rabbit polyclonal anti-xCT (1:1000)	Cell Signaling Technology	Cat#98051; RRID: AB_2800296
Rabbit monoclonal anti-GPX4 (1:1000)	Abcam	Cat#ab125066; RRID: AB_10973901
Rabbit monoclonal anti-VCP (1:10000)	Abcam	Cat#ab109240; RRID: AB_10862588
Horse anti-mouse-IgG-HRP (1:3000)	Cell Signaling Technology	Cat# 7076S; RRID: AB_330924
Goat anti-rabbit-IgG-HRP (1:3000)	Cell Signaling Technology	Cat# 7074S; RRID: AB_2099233
Chemicals, peptides, and recombinant proteins		
cystathionine	Cayman Chemical	Cat#16061
(1S,3R)-RSL3 (RSL3)	Cayman Chemical	Cat#19288
ML162	Cayman Chemical	Cat#20455
ML210	Cayman Chemical	Cat#23282
FIN56	Cayman Chemical	Cat#25180
$FINO_2$	Cayman Chemical	Cat#25096
iFSP1	Cayman Chemical	Cat#29483
erastin	Sigma-Aldrich	Cat#329600
L-buthionine sulfoximine (BSO)	Sigma-Aldrich	Cat#B2515
L-cysteine	Sigma-Aldrich	Cat#C7352
D-cysteine	Sigma-Aldrich	Cat#30095
(Z)-4-hydroxytamoxifen (Tam)	Sigma-Aldrich	Cat#H7904
WIN 62,577	Sigma-Aldrich	Cat#W104
β-mercaptoethanol (β-ME)	Sigma-Aldrich	Cat#M7522
cysteamine	Sigma-Aldrich	Cat#M9768
DL-dithiothreitol (DTT)	Sigma-Aldrich	Cat#D0632
tris(2-carboxyethyl)phosphine (TCEP)	Sigma-Aldrich	Cat#C4706
L-cystine	Sigma-Aldrich	Cat#C7602
L-glutathione (GSH)	Sigma-Aldrich	Cat#PHR1359
L-glutathione disulfide (GSSG)	Sigma-Aldrich	Cat#PHR2461
N-acetyl-L-cysteine (NAC)	Merck Millipore	Cat#1124220100
N-acetyl-L-cysteine (NAC)	Carl Roth	Cat#4126.1
N-acetyl-D-cysteine (D-NAC)	MedChemExpress	Cat#HY-136386
liproxstatin-1 (Lip-1)	Selleck Chemicals	Cat#S7699
sulfasalazine	VWR	Cat#S0883
β-mercaptoethanol (β-ME)	Thermo Fisher	Cat#31350010
viFSP1	Vitas-M Laboratory	Cat#STK626779
icFSP1	Nakamura et al.[27]	N/A
Experimental models: Cell lines		
Mouse: Tam-inducible *Gpx4*$^{-/-}$ immortalized fibroblasts (Pfa1 cells)	Seiler et al.[22]	N/A

(*Continued on next page*)

Please cite this article in press as: Zheng et al., *N*-acetyl-L-cysteine averts ferroptosis by fostering glutathione peroxidase 4, Cell Chemical Biology (2025), https://doi.org/10.1016/j.chembiol.2025.04.002

CellPress
OPEN ACCESS

Continued

REAGENT or RESOURCE	SOURCE	IDENTIFIER
Mouse: *Gpx4*^{KO} Pfa1	Nakamura et al.[23]	N/A
Mouse: *Gpx4*^{KO} *hFSP1*^{OE} Pfa1	Nakamura et al.[27]	N/A
Mouse: *Slc7a11*^{KO} Pfa1	This paper	N/A
Mouse: *Gclc*^{KO} Pfa1	This paper	N/A
Mouse: *Gclc*^{KO} Pfa1 (adapted)	This paper	N/A
Mouse: *mSlc7a11*^{OE} Pfa1	This paper	N/A
Mouse: *mSlc7a11*^{OE} *Gpx4*^{KO} Pfa1	This paper	N/A
Mouse: *Gpx4*^{KO} Pfa1 + FSH-hGPX4	This paper	N/A
Mouse: *Gpx4*^{KO} Pfa1 + FSH-hGPX4-U46S	This paper	N/A
Human: HT1080	ATCC	Cat#CCL-121
Human: *SLC7A11*^{KO} HT1080	Zheng et al.[12]	N/A
Human: *FSP1*^{KO} HT1080	Mishima et al.[32]	N/A
Human: *GPX4*^{KO} *hFSP1*^{OE} HT1080	Doll et al.[25]	N/A
Oligonucleotides		
mSlc7a11 CRISPR/Cas9 targeting sequence GAAGAGACACAAGTCTAATG and TGGAGATGCAGATTGCAAGG	This paper	N/A
mGclc CRISPR/Cas9 targeting sequence TGGGTCTCTTCCCAGCTCAG and GTACCTTGGACAGCGGAATG	This paper	N/A
mouse *Slc7a11* qPCR forward primer CTACTGCTGTGATATCCCTG	This paper	N/A
mouse *Slc7a11* qPCR reverse primer CACTCGTGCTATTTAGGACC	This paper	N/A
mouse *Gapdh* qPCR forward primer GGTTGTCTCCTGCGACTTCA	This paper	N/A
mouse *Gapdh* qPCR reverse primer TGGTCCAGGGTTTCTTACTCC	This paper	N/A
human *SLC7A11* qPCR forward primer GCAGCTACTGCTGTGATATC	This paper	N/A
human *SLC7A11* qPCR reverse primer CAGAATTGCTGTGAGCTTGC	This paper	N/A
human *GAPDH* qPCR forward primer GATCATCAGCAATGCCTCCT	This paper	N/A
human *GAPDH* qPCR reverse primer CAGGGATGATGTTCTGGAGA	This paper	N/A
Recombinant DNA		
Plasmid: lentiCRISPR v2 neo	Stringer et al.[33]	Cat#98292; Addgene
Plasmid: lentiCRISPR v2 blast	Stringer et al.[33]	Cat#98293; Addgene
Plasmid: p442-FSH-hGPX4 (NM_001367832.1)-IRES-blast	This paper	N/A
Plasmid: p442-FSH-hGPX4-U46S (tga>agc)-IRES-blast	This paper	N/A
Plasmid: p442-mSlc7a11-IRES-blast	This paper	N/A
Software and algorithms		
GraphPad Prism v10	GraphPad Software	https://www.graphpad.com/features
VBC Score	Michlits et al.[34]	https://www.vbc-score.org
SCIEX OS Software 3.3.1	SCIEX	https://sciex.com/support/software-support/software-downloads

Please cite this article in press as: Zheng et al., *N*-acetyl-L-cysteine averts ferroptosis by fostering glutathione peroxidase 4, Cell Chemical Biology (2025), https://doi.org/10.1016/j.chembiol.2025.04.002

EXPERIMENTAL MODEL AND STUDY PARTICIPANT DETAILS

Cell lines

The Tam-inducible *Gpx4* knockout mouse immortalized fibroblasts Pfa1 [referred to as WT Pfa1],[22] *Gpx4*^{KO} Pfa1,[23] *Gpx4*^{KO} *hFSP1*^{OE} Pfa1,[27] human fibrosarcoma HT1080, *SLC7A11*^{KO} HT1080,[12] *FSP1*^{KO} HT1080[32] and *GPX4*^{KO} *hFSP1*^{OE} HT1080[25] were reported previously. *Slc7a11*^{KO}, *Gclc*^{KO} and *mSlc7a11*^{OE} Pfa1 cells were generated from WT Pfa1 cells, and *mSlc7a11*^{OE} *Gpx4*^{KO} Pfa1 cells were generated from *mSlc7a11*^{OE} Pfa1 cells following the methods described below. Cells were maintained in DMEM (#21969035) supplemented with 10% fetal bovine serum (FBS), 2 mM glutamine and 1% penicillin-streptomycin from Thermo Fisher unless otherwise specified. To maintain *Gclc*^{KO}, *Gpx4*^{KO} and *mSlc7a11*^{OE} *Gpx4*^{KO} Pfa1 cells, 100 nM Lip-1 was supplemented to the culture media. To maintain *SLC7A11*^{KO} HT1080 cells and *Slc7a11*^{KO} Pfa1 cells, 50 μM β-ME was supplemented to the culture media. For certain experiments, cystine-free media (#21013024, Thermo Fisher) supplemented with 10% FBS, 2 mM glutamine, 1% penicillin-streptomycin and 200 μM methionine was used. All cells were cultured at 37°C with 5% CO_2 and verified to be negative for mycoplasma.

METHOD DETAILS

Reagents

Reagents used in this work include cystathionine (#16061), *(1S,3R)*-RSL3 (RSL3) (#19288), ML162 (#20455), ML210 (#23282), FIN56 (#25180), $FINO_2$ (#25096) and iFSP1 (#29483) from Cayman Chemical; erastin (#329600), L-buthionine sulfoximine (BSO) (#B2515), L-cysteine (#C7352), D-cysteine (#30095), (Z)-4-hydroxytamoxifen (Tam) (#H7904), WIN 62,577 (#W104), β-mercaptoethanol (β-ME) (#M7522), cysteamine (#M9768), DL-dithiothreitol (DTT) (#D0632), and tris(2-carboxyethyl)phosphine (TCEP) (#C4706) from Sigma-Aldrich; *N*-acetyl-L-cysteine (NAC) (#1124220100) from Merck Millipore; *N*-acetyl-D-cysteine (D-NAC) (#HY-136386) from MedChemExpress, liproxstatin-1 (Lip-1) (#S7699) from Selleck Chemicals; sulfasalazine (#S0883) from VWR, β-ME (#31350010) from Thermo Fisher; viFSP1 (#STK626779) from Vitas-M Laboratory; and icFSP1 synthesized by Intonation Research Laboratories.[27]

The following reagents were used for LC-MS/MS analysis:L-cystine (#C7602), L-cysteine (#C7352), L-glutathione (GSH) (#PHR1359), L-glutathione disulfide (GSSG) (#PHR2461) and *N*-ethylmaleimide (NEM) (#04259) from Sigma-Aldrich, *N*-acetyl-L-cysteine (NAC) (#4126.1) from Carl Roth, L-glutathione-$^{13}C_2$,^{15}N (#CNLM-6245-0) and L-glutathione disulfide-$^{13}C_2$,^{15}N (#CNLM-8782-0) from Cambridge Isotope Laboratories, *N,N'*-diacetyl-L-cystine (#17596), L-cysteine-^{15}N-D3 (#34838) andDL-cystine-D4 (#30902) from Cayman Chemical, LC-MS grade water (#455), methanol (#1428) and acetonitrile (#2697) from Th. Geyer, and ammonium formate (#55674) and formic acid (#94318) from Honeywell.

Generation of knockout cell lines

Slc7a11^{KO} and *Gclc*^{KO} Pfa1 cells were generated using CRISPR/Cas9 system-based technology. In brief, two single guide RNAs were designed for each gene (*Slc7a11* and *Gclc*) using the platform https://www.vbc-score.org/.[34] The targeting sequence were "GAAGAGACACAAGTCTAATG" and "TGGAGATGCAGATTGCAAGG" for *Slc7a11*, and "TGGGTCTCTTCCCAGCTCAG" and "GTACCTTGGACAGCGGAATG" for *Gclc*. The single guide RNAs were cloned in the *BsmB*I-digested lentiCRISPR v2 neo and lentiCRISPR v2 blast vectors (#98292 and #98293, Addgene) respectively,[33] and then co-lipofected into WT Pfa1 cells using the X-tremeGene HP DNA Transfection Reagent (#06366236001, Sigma-Aldrich). After 24 hours incubation, transfected cells were trypsinized and selected with both geneticin (800 μg/ml) and blasticidin (10 μg/ml) in 10-cm dishes for over one week. For *Slc7a11*^{KO} and *Gclc*^{KO}, 50 μM β-ME and 1 μM Lip-1 were supplemented to the culture media, respectively. Cells that survived the selection were collected and 100 cells were plated on three 96-well plates to allow formation of single cell clones. *Slc7a11*^{KO} and *Gclc*^{KO} single cell clones were verified by β-ME and Lip-1 removal, respectively (the knockout cells would die in the absence of supplementation). The selected *Gclc*^{KO} single cell clone was further verified by immunoblotting. To obtain *Gclc*^{KO} (adapted) cells, the concentration of Lip-1 supplemented to the *Gclc*^{KO} single cell clone was decreased in a stepwise approach alone with cell passage. After a few weeks of adaptation, the cells could survive and proliferate infinitely in the absence of Lip-1.

Overexpression of xCT by viral transduction

Mouse *Slc7a11* cDNA was cloned and inserted into the viral expression vector p442-IRES-blast[25] using In-Fusion cloning system (#638948, Takara Bio). Human HEK293T cells from ATCC were used to produce lentiviral particles. Briefly, mouse xCT expression plasmid was co-lipofected with an envelope plasmid pHCMV-EcoEnv (#15802, Addgene) and a packaging plasmid psPAX2 (#12260, Addgene) into HEK293T cells using transfection reagent PEI MAX (#24765, Polysciences). Supernatants containing viral particles were collected 2-3 days later and filtered through a 0.45-μm PVDF filter (#SLHV033RS, Millipore). For viral transduction, WT Pfa1 cells were seed on a 12-well plate with the virus-containing supernatant supplemented with protamine sulfate (10 μg/ml). After 24 hours incubation, transfected cells were trypsinized and selected with blasticidin (10 μg/ml) in a 10-cm dish for over one week. To generate *mSlc7a11*^{OE} *Gpx4*^{KO} Pfa1 cells, *mSlc7a11*^{OE} Pfa1 cells were treated with Tam for 72 hours in the presence of 1 μM Lip-1. Subsequently, single cell clones were generated following the method described above and then verified by immunoblotting.

qPCR analysis

Total RNA extraction from Pfa1 and HT1080 cells was performed using RNeasy Mini Kit (#74104, Qiagen). Reverse transcription was performed using QuantiTect Reverse Transcription Kit (#205313, Qiagen). qPCR reactions were performed on qTOWER3 G

Please cite this article in press as: Zheng et al., *N*-acetyl-L-cysteine averts ferroptosis by fostering glutathione peroxidase 4, Cell Chemical Biology (2025), https://doi.org/10.1016/j.chembiol.2025.04.002

(Analytikjena) using PowerUp SYBR Green Master Mix (#A25742, Thermo Fisher). The following primers were used: mouse *Slc7a11* (5'-CTACTGCTGTGATATCCCTG-3' and 5'-CACTCGTGCTATTTAGGACC-3'), mouse *Gapdh* (5'-GGTTGTCTCCTGCGACTTCA-3' and 5'-TGGTCCAGGGTTTCTTACTCC-3'), human *SLC7A11* (5'-GCAGCTACTGCTGTGATATC-3' and 5'-CAGAATTGCTGT GAGCTTGC-3') and human *GAPDH* (5'-GATCATCAGCAATGCCTCCT-3' and 5'-CAGGGATGATGTTCTGGAGA-3').

Immunoblotting

Cells were lysed in LCW lysis buffer (0.5% Triton-X-100, 0.5% sodium deoxycholate salt, 150 mM NaCl, 20 mM Tris-HCl, 10 mM EDTA, 30 mM Na-pyrophosphate) containing protease and phosphatase inhibitor cocktail (#04693116001 and #4906837001, both Roche), and cell debris were removed by centrifugation (12,000×g, 4°C, 20 min). The supernatant was supplemented with 6× SDS sample buffer (375 mM Tris-HCl pH 6.8, 9% SDS, 50% glycerol, 9% β-mercaptoethanol and 0.03% bromophenol blue) and heated at 99°C (50°C for xCT) for 5 min. Immunoblotting was performed with 12% SDS-PAGE gel and PVDF membrane. Primary antibodies against glutamate-cysteine ligase catalytic subunit (GCLC) (1:200, #sc-22755, Santa Cruz), cystathionine γ-lyase (CTH) (1:1000, #GTX113409, GeneTex), mouse xCT (1:1000; #98051, Cell Signaling Technology), GPX4 (1:1000; #ab125066, Abcam), and valosin containing protein (VCP) (1:10000; #ab109240, Abcam) were used.

Cell viability

Pfa1 and HT1080 cells were seeded on 96-well plates at a density of 1,100 and 1,600 cells/well, respectively, for the 24 hours treatments, and 300 and 500 cells/well for the 72 hours treatments. The next day, cells were treated with compounds as indicated. For experiments using cystine-free media or with β-ME/Lip-1 removal, cells were washed with PBS before the treatment. For experiments using cystine-free media supplemented with cystathionine, cells were seeded as such rather than in normal media. Cell viability was assessed using resazurin (final concentration: 20 μg/ml) as an indicator of viable cells.

Cell morphology

Pfa1 and HT1080 cells were seeded on 6-well plates at a density of 20,000 and 30,000 cells/well, respectively. For experiments with Tam treatment, cells were seeded at a density of 10,000 cells/well. Cells were treated as described above. Static brightfield images of cells were captured using an ECLIPSE Ts2 microscope (Nikon).

Living cell counting

Pfa1 and HT1080 cells were seeded on 6-well plates as described above. On the day of harvest, cells were trypsinized and diluted with culture media. After brief vortexing, 100 μL of the cell suspension was collected and mixed with 100 μL of 0.4% Trypan Blue solution (#T10282, Invitrogen) to stain for dead cells. Viable cells were then counted using a hemocytometer.

GPX4 activity assay

This assay was performed based on the reported method with slight modification.[23,35] Briefly, 16:0-20:4 phosphatidylcholine hydroperoxide (PCOOH) was prepared by photo-oxidation of 1-palmitoyl-2-arachidonoyl-*sn*-glycero-3-phosphocholine (16:0-20:4 PC, #850459C, Avanti Research). The GPX4 enzyme was collected from *Gpx4*^{KO} Pfa1 cells overexpressing FSH-tagged hGPX4_WT or hGPX4_U46S by affinity purification. The FSH-tagged hGPX4_WT plasmid was generated by recloning the sequence from a 141-IRES-puro vector as previously described,[23] into a p442-IRES-blast vector. The FSH-tagged hGPX4_U46S plasmid was then generated from the FSH-hGPX4_WT plasmid using site-directed mutagenesis. The enzymatic reaction was performed in 96 well plates in the presence of 4 μL of affinity-purified GPX4 (final concentration 18 nM), 2 μL of PCOOH (final concentration 10 μM) dissolved in 0.1% Triton X-100 and 4 μL of potential GPX4 reducing substrates as indicated. After 1 h of incubation at 37°C, the reaction was stopped by transferring 5 μL of sample into 495 μL of methanol, which was then subjected to an LC-MS/MS system [QTRAP 7500 tandem mass spectrometer (SCIEX) equipped with an Exion LC system (SCIEX)] to determine the remaining PCOOH[36] and the oxidized products of NAC and D-NAC as described below.

LC-MS/MS

Detection of the oxidized products of NAC and D-NAC in the GPX4 activity assay

To detect the oxidized products of NAC and D-NAC in the GPX4 activity assay, 10 μL of the diluted reaction sample was mixed with 80 μL of methanol/water (80:20, v/v) containing 25 mM NEM and 10 mM ammonium formate, along with 10 μL of an internal labeled standard mixture. The internal standard mixture included 15 μM L-cysteine-^{15}N-D_3, 20 μM DL-cystine-D_4, 10 μM L-glutathione-$^{13}C_2$,^{15}N, and 50 μM L-glutathione disulfide-$^{13}C_2$,^{15}N. The samples were then subjected to LC-MS/MS analysis.

Measurement of intracellular cysteine and GSH levels

To measure intracellular cysteine and GSH levels, cells were seeded on 10 cm plates at a density of 30–50% and treated as indicated the following day. After treatment, cells were washed with PBS, trypsinized, resuspended in PBS, and divided equally into two fractions. One fraction was pelleted for subsequent protein quantification using the Pierce BCA Protein Assay Kit (#23225, Thermo Scientific). The other fraction was resuspended in 1 mL of methanol/water (80:20, v/v) containing 25 mM NEM and 10 mM ammonium formate. The cells were then transferred to Precellys Lysing Kit tubes (#P000912-LYSK1-A, Bertin Technologies) and homogenized using a Retsch MM400 mixer mill (frequency: 30/s, duration: 5 min), followed by centrifugation (550 ×g, 4°C, 10 min). Subsequently,

Please cite this article in press as: Zheng et al., *N*-acetyl-L-cysteine averts ferroptosis by fostering glutathione peroxidase 4, Cell Chemical Biology (2025), https://doi.org/10.1016/j.chembiol.2025.04.002

20 μL of the supernatant were collected and mixed with 80 μL of methanol/water containing NEM and ammonium formate, along with 10 μL of the internal labeled standard mixture as described above. The samples were then subjected to LC-MS/MS analysis.

LC-MS/MS analysis

LC-MS/MS analysis was performed using the same system as described for the GPX4 activity assay. For HPLC, a silica-based C18 column (Atlantis T3, 3 × 150 mm, 3 μm particle size; Waters, Milford, MA, USA) was used for reversed-phase separation. The flow rate was set to 300 μL/min, and the column temperature was maintained at 40°C. The injection volume was 1 μL. The chromatographic run began with 85% mobile phase A (water, 5 mM ammonium formate, 0.1% formic acid) for 2 minutes, followed by a gradient from 15% to 100% mobile phase B (acetonitrile, 0.1% formic acid) over 6 min. A cleaning step at 100% mobile phase B and sufficient column re-equilibration under initial gradient conditions resulted in a total run time of 12.5 min.

For mass spectrometry, electrospray ionization (ESI) was operated in positive ion mode (source temperature: 550°C, spray voltage: 2500 V, ion source gas 1: 65 psi, ion source gas 2: 70 psi, curtain gas: 45 psi). Data acquisition was performed in scheduled multiple reaction monitoring (sMRM) mode according to the transition of precursor ions to products. All peaks were integrated using the SCIEX OS software (version 3.3.1) and the AutoPeak algorithm. Quantification was performed based on the signal intensity ratios of each analyte of interest to its corresponding labeled analog. For this purpose, calibration solutions were prepared as standard mixtures of the metabolites of interest, with equal amounts of labeled standards added. NAC and $(NAC)_2$ were quantified using labeled cysteine as the internal standard. Finally, $(NAC)_2$ and $(D\text{-}NAC)_2$ concentrations were multiplied by 100 to reflect their original concentrations in the reaction system. Cysteine and GSH concentrations were normalized to total protein content.

QUANTIFICATION AND STATISTICAL ANALYSIS

Statistical details for individual experiments are provided in the corresponding figure legends. No formal statistical analysis was conducted in this study. Graphs were created using GraphPad Prism v10 (GraphPad Software).